

Supporting Information:

Enhanced Capacity and Lower Mean Charge Voltage of Li-Rich Cathodes for Lithium Ion Batteries Resulting from Low-Temperature Electrochemical Activation

Evan M. Erickson,^a Florian Schipper,^a Ruiyuan Tian,^a Ji-Yong Shin,^b Christoph Erk,^b Frederick-Francois Chesneau,^b Jordan Lampert,^b Boris Markovsky,^a and Doron Aurbach^a

^a Department of Chemistry, Faculty of Exact Sciences, Bar-Ilan University, Ramat-Gan, 5290002 Israel

^b Badische Anilin und Soda Fabrik (BASF), Ludwigshafen am Rhein, Rheinland-Pfalz, Germany

1. Structural Information of the Li-rich Material

A SEM micrograph depicting the morphology of the $0.35\text{LiMn}_2\text{O}_3 \cdot 0.65\text{Li}[\text{Mn}_{0.45}\text{Ni}_{0.35}\text{Co}_{0.20}]\text{O}_2$ cathode material is presented in Figure S 1, showing ball-shaped particles with around 5 - 10 μm in diameter.

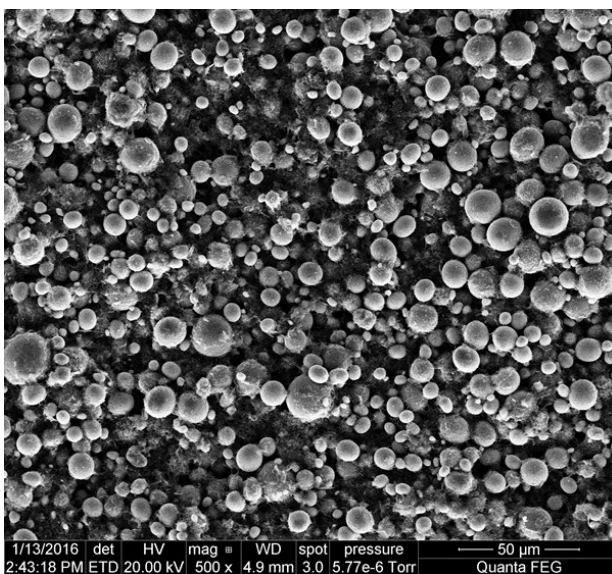


Figure S 1: SEM micrograph of an uncycled $0.35\text{LiMn}_2\text{O}_3 \cdot 0.65\text{Li}[\text{Mn}_{0.45}\text{Ni}_{0.35}\text{Co}_{0.20}]\text{O}_2$ electrode.

The XRD pattern for uncycled Li-rich powder is presented in Figure S 2 with the resultant derived lattice parameters (Table S 1).

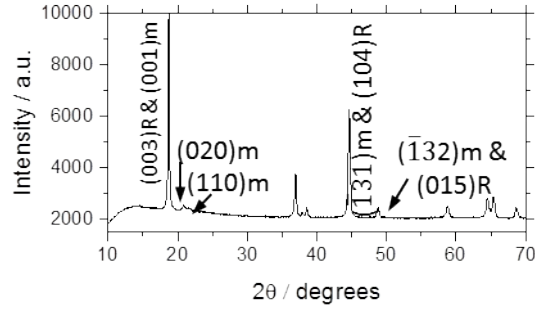


Figure S 2: XRD pattern from pristine, uncycled Li-rich $0.35\text{LiMn}_2\text{O}_3 \cdot 0.65\text{Li}[\text{Mn}_{0.45}\text{Ni}_{0.35}\text{Co}_{0.20}]\text{O}_2$ powder with some reflections indicated.

Material	Monoclinic phase	Rhombohedral phase (in terms of hexagonal cell)	Rp value
Pristine (uncycled)	$a=4.929(4) \text{ \AA}$, $b=8.522(9) \text{ \AA}$, $c=5.029(0) \text{ \AA}$, $\beta =109.19^\circ \text{ \AA}$	$a=2.857(3) \text{ \AA}$, $c=14.259(6) \text{ \AA}$	2.79%

Table S 1: Lattice parameters of monoclinic Li_2MnO_3 ($C2/m$) and rhombohedral ($R\bar{3}m$) components of pristine (uncycled) Li-rich $0.35\text{Li}_2\text{MnO}_3 \cdot 0.65\text{LiNi}_{0.35}\text{Mn}_{0.45}\text{Co}_{0.20}\text{O}_2$ powder.

2. Cycling of cells

All cycling results in this manuscript represent the average of 3 - 4 coin cells (vs. Li counter electrodes) with standard deviations used as error bars to ensure confidence in our results. The cells whose results are depicted in Fig. 1 were first cycled to 4.7 V at C/15 (1C defined as 250 mAhg⁻¹) for the first cycle, with a constant voltage step for 3 hrs. The second cycle was performed at a C/10 rate, with this and all subsequent cycles charged to only 4.6 V, utilizing a 30 min constant voltage step. The first two cycles were the “activation steps,” performed at 0, 15, 30 or 45 °C, indicated in the legends of Fig. 1 & 2. After the two-cycle activation steps, cells were either cycled at 30 °C (Fig. 1) or 45 °C. The cycling procedure includes a rate capability measurement at first up to 4C (with the same charge and discharge rates). The rate capability test was followed by 3 cycles at C/10 and with the remaining 80 cycles at C/3.

Coin cells were fabricated with 3:7 EC:EMC, 1 M LiPF₆ electrolyte, Celgard 2500 polypropylene separators, and ~3 mg/cm² active Li-rich material electrodes. The electrodes are comprised of 80 % active material, 10 % Solef 5140 PVDF, 5 % C black and 5 % KS6 graphite.

3. Differential capacity vs. V plots, over long term cycling.

Figure S 3 depicts the dQ/dV curves of electrodes throughout long term cycling. The Li^+ extraction from the TM layer is characterized by the most intense peak for the material activated at low T. In the figure, Peak 2 corresponds to Li^+ extraction from the TM layer, Peak 3 corresponds to Li^+ extraction from the Li^+ layer, and peak 4 is likely related to spinel phase redox that is formed due to partial layered-to-spinel transformation in Li-rich electrode materials.

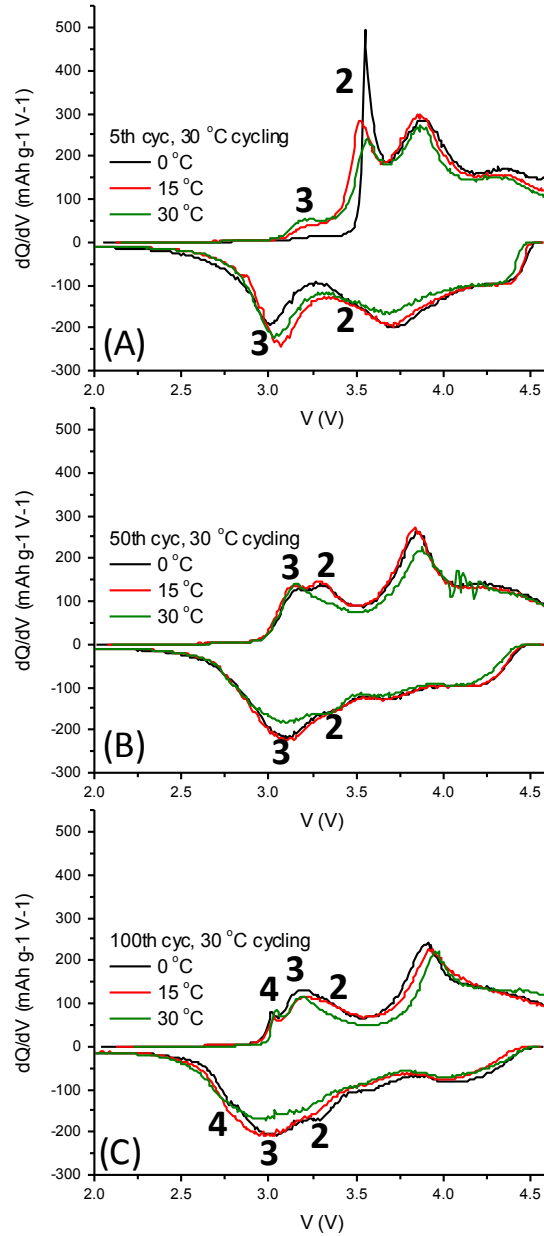


Figure S 3: Differential capacity vs. voltage plots of the Li-rich material electrodes activated at 0 – 30 °C, cycled at 30 °C, over 100 cycles.